

The survival of subhaloes in galaxies and galaxy clusters

Eelco van Kampen

Institute for Astronomy, University of Edinburgh, Royal Observatory, Blackford Hill, Edinburgh EH9 3HJ, evk@roe.ac.uk

Accepted ... Received ...; in original form ...

ABSTRACT

This paper discusses physical and numerical disruption processes acting on subhaloes in galaxy haloes and in galaxy cluster haloes, and compare the effects of these processes on the subhalo abundance within both types of haloes. N-body simulations with a resolution high enough not to suffer from overmerging (subhalo disruption due to numerical processes) show a high abundance of subhaloes in both galaxies and in galaxy clusters. However, observations seem to show a high subhalo abundance in galaxy clusters only. Thus, it appears that too many subhaloes survive in simulated galaxy haloes.

There are five main causes for this apparent galaxy subhalo problem. The most radical one is a change to a cosmology in which structure formation is not hierarchical below the galaxy halo mass scale. If this is unacceptable, four causes remain, of which the most important one appears to be that dynamical friction is not properly simulated yet, not even for the highest resolution simulations to date, resulting in an ‘undermerging’ problem. The other causes are (numerical) overmerging, differences in the timing of halo formation and merging in hierarchical structure formation, and significant differences in mass-to-light ratios. The net effect of these four causes is that galaxies have a relatively low abundance of subhaloes, i.e. dwarfs, while at the same time a large number of field dwarf galaxies can exist which are dark enough to be missed observationally.

Key words: galaxies: evolution - dark matter - large-scale structure of Universe

1 INTRODUCTION

Hierarchical formation of structure in the universe implies the formation of galaxy and galaxy cluster haloes through accretion and merging of smaller entities. These entities usually survive as identifiable subhaloes for some time. The topic of this paper is the difference in the fate of subhaloes in galaxy clusters and in galaxies, but also the mismatch between the high abundance of subhaloes in galaxies simulated for a hierarchical structure formation model dominated by Cold Dark Matter (e.g. Moore et al. 1999; Klypin et al. 1999b) and the observed low abundance of dwarf galaxies (e.g. Mateo 1998).

For the modelling of structure formation one usually employs N-body simulations, in which the matter distribution is sampled by discrete particles. Haloes are thus modelled as groups of N-body particles, which can merge, be disrupted, or survive intact, depending on the physical processes that are in operation, like dynamical friction, tidal stripping, and others. However, merging and disruption can also be due to purely numerical processes, which are especially troublesome for subhaloes consisting of small numbers of particles (van Kampen 2000 and references therein).

In order to distinguish between numerical and physical causes for disruption or survival of subhaloes, one approach

is to look at simulations of the same matter distribution at different resolutions. If a specific effect is seen at two different resolutions, it is likely to be physical, whereas if it is only seen to operate for the lower resolution simulation, it must be a numerical effect. This test was first performed by van Kampen (1995), but the simulations were not yet of sufficient resolution to clearly differentiate between physical and numerical effects, even though the numerical effects appeared to dominate. Another approach is to set up experiments where one of the effects is artificially eliminated. Such tests show that numerical effects dominate for small subhaloes (van Kampen 2000).

Recently several research groups used simulations with a higher resolution to look at this problem (Klypin et al. 1999a; Ghinga et al. 1998, 1999; Moore et al. 1999; Okamoto & Habe 1999). However, different group finders and different definitions for disruption times were used, so a direct comparison of the results is not possible. Still, the consensus is that increasing the number of particles overcomes, at least partially, the overmerging problem. Unfortunately, for N-body simulations on a cosmological scale, this requires the use of very many particles (on the order of 10^9), which is not practical. Furthermore, for the smallest subhaloes the overmerging problem simply remains, as the disruption timescale depends mainly on the number of particles in the subhalo.

arXiv:astro-ph/0008453v1 29 Aug 2000

Now that recent simulations manage to partially resolve the overmerging problem, a new problem, rather ironically, has surfaced: for some physical systems *too many* subhaloes survive as compared to observed abundances. Moore et al. (1999) and Klypin et al. (1999b) find that hierarchical formation models predict many more galaxy subhaloes, i.e. dwarf subhaloes, than observed. Thus, the question is whether cosmological initial conditions are such that few dwarf galaxies form in the first place, or that they are easily destroyed within our Galaxy *and* not replaced. On a larger scale, clusters of galaxies do contain an abundance of subhaloes, namely its member galaxies. If these are destroyed as easily as galaxy subhaloes, then they should be replaced at low redshift by newly accreted galaxies. Otherwise, the only possibility is that subhaloes need to be disrupted more easily in galaxy haloes than in galaxy cluster haloes.

The aim of this paper is to establish what causes the difference in subhalo abundance between galaxies and galaxy clusters, and whether the survival or disruption of subhaloes in simulated embedding haloes is effected by numerical or physical processes. In Section 2 the various numerical and physical processes acting on subhaloes are listed and discussed, and quantitative estimates for the corresponding disruption timescales are given for subhaloes in galaxy cluster and galaxy haloes. Possible reasons for the discrepancy of the subhalo abundance in simulations and observations are discussed in Section 3. Specific problems with the modelling of dynamical friction are examined in Section 4. The consequences of the timing of hierarchical structure formation are discussed in Section 5. Finally, a summary with conclusions is provided in Section 6.

2 SUBHALO DISRUPTION PROCESSES

2.1 Definitions

Before proceeding to discuss disruption process, it is useful to clarify the associated terminology. A *halo* is defined as a collapsed and virialized density maximum, whereas a halo that contains *subhaloes* is denoted as an *embedding halo*, or as a *parent* halo. The term *overmerging* is used for the numerical processes that artificially merge haloes and subhaloes in an N-body model by dissolving the subhalo. The term *undermerging* is introduced here to express the inability to model processes that should cause merging or disruption. Thus, the term *merging* only denotes merging due to physical processes that actually happen in the numerical simulation used.

2.2 Numerical disruption processes

Most galaxies and clusters of galaxies are modelled using N-body simulations, in which discrete particles sample the true density distribution. The number of N-body particles sets the resolution of the simulation. If the resolution is too low, i.e. too few particles are used, discreteness effects become important, even for *softened* particles. Two-body interactions can *evaporate* a halo completely. More importantly, subhaloes can be dissolved by *two-body heating* or *tidal heating*. These two processes are both driven by the particles of the embedding halo, but tidal heating is driven by encounters between embedding halo particles and collisionless

subhaloes, while two-body heating is driven by two-body encounters between embedding halo particles and individual subhalo particles.

The timescales for these processes are expressed in terms of the *crossing time* $t_c \equiv r/v$, where r is the *half-mass radius*, and v the *typical velocity* (usually taken to be equal to the velocity dispersion). The *two-body evaporation* timescale for either a halo or a subhalo is

$$t_{\text{evap}} \approx 30 \frac{N}{\ln N} \frac{r}{v} \quad (1)$$

(e.g. Binney & Tremaine 1987), where N is the number of particles in the (sub)halo. The *particle-subhalo two-body heating* timescale is given by (van Kampen 1995, 2000)

$$t_{\text{heat}} \approx 0.1 \frac{N_s}{\ln(r_h/2\epsilon)} \frac{r_h}{r_s} \frac{r_h}{v_h}, \quad (2)$$

where the subscripts s and h indicate subhalo and embedding halo respectively. Finally, the timescale for *particle-subhalo tidal disruption* (or *impulsive disruption*) is given by van Kampen (2000)

$$t_{\text{tidal}} \approx 1.3 N_s \left(\frac{r_p}{r_s} \right)^{\frac{1}{2}} \frac{r_h}{r_s} \frac{r_h}{v_h} \quad (3)$$

for isothermal subhaloes, and

$$t_{\text{tidal}} \approx 0.5 N_s \frac{r_h}{r_s} \frac{r_h}{v_h} \quad (4)$$

for Plummer subhaloes. In both cases, r_p is taken to be equal to the softening length ϵ . Because both r_s/r_p and r_h/r_s are of order ten, and $\ln(r_h/2\epsilon)$ is around 5, the two disruption times are approximately $0.2N_s$ and $5N_s$ embedding halo crossing times respectively. Both timescales are smaller than the evaporation timescale, but particle-subhalo two-body heating is clearly the dominant effect. Derivations and a more detailed discussion are published elsewhere (van Kampen 2000).

Softening alleviates the problem of two-body effects somewhat, but softened particle groups are more extended and less strongly bound (van Kampen 1995). This re-enhances two-body disruption processes, which are more efficient for more extended subhaloes, as shown below. More importantly, softening effects the timescales for some of the *physical* disruption processes as well, especially those that depend on the subhalo size.

2.3 Physical disruption processes

2.3.1 Mean tidal field of embedding halo

One obvious physical mechanism operating on subhaloes is heating, stripping, or even disruption by the mean tidal field of the embedding halo. Various estimates and tests for the timescale and associated tidal radius exist in the literature (e.g. Allen & Richstone 1988; Heisler & White 1990; van Kampen 1995; Moore et al. 1996; Klypin et al. 1999). Unfortunately, the tidal disruption timescale sensitively depends on the density profile of the embedding halo and the actual orbit of the subhalo. Tidal disruption is most efficient on circular orbits near the core radius of the embedding halo, but less so on radial orbits where the subhalo spends most of its time outside the ‘danger zone’, a broad shell around the core where the tidal limit is smallest. Such subhaloes

lose mass due to tidal shocks which are less efficient than a constant tidal force along a circular orbit (e.g. Moore et al. 1996).

Thus, it is unlikely that the mean tidal field completely destroys a subhalo, usually the subhalo is only stripped down to its tidal radius. If the mean tidal field destroys subhaloes, this should have been seen in high-resolution simulations. However, most authors find that a large fraction of subhaloes survive as identifiable entities, even though they can suffer significant mass loss and are tidally limited.

As pointed out by van Kampen (1995), groups of softened N-body particles are more extended and less bound than physical haloes, and are therefore not only more vulnerable to the mean tidal field, but also to two-body heating. Furthermore, both processes work in the same direction and therefore accelerate each other. This complicates the study of tidal processes and their effects on the evolution of subhaloes. One solution is to take a fixed potential for the embedding halo, and only use particles for the subhalo (e.g. Heisler & White 1990; Moore et al. 1996; van Kampen 2000). The alternative solution is to increase the resolution of the simulation; if a sufficient number of particles is employed, the subhalo will not be destroyed by numerical processes, but tidal processes will still be artificially enhanced.

2.3.2 Subhalo-subhalo tidal heating

N-body particles are relatively massive, and therefore tidally heat subhaloes (Moore et al. 1996; van Kampen 2000), a process which is independent of the number of particles in the subhalo, as subhaloes are assumed to be collisionless for this process. Just like N-body particles can tidally disturb subhaloes, subhaloes also tidally disturb each other. Moore et al. (1996) estimate a timescale for this process by scaling the timescale for tidal heating of subhaloes by individual N-body particles. However, there are two problems with their estimate: their particle-subhalo timescale estimate is incorrect, and their scaling to subhalo-subhalo tidal heating misses a term.

The first problem is that the estimate for the particle-subhalo tidal heating timescale is longer than the estimate Moore et al. give by a factor of $13(r_s/r_p)^{3/2}$ for isothermal subhaloes, or $5(r_s/\epsilon)^2$ for Plummer subhaloes (see van Kampen 2000). For isothermal subhaloes, the corrected timescale estimate is

$$t_{\text{dis}} \approx 1100 \left(\frac{v_h}{1700 \text{ km s}^{-1}} \right) \left(\frac{\epsilon^{1/4} r_s^{3/4}}{10 \text{ kpc}} \right)^2 \left(\frac{10^9 M_\odot}{m_p} \right) \text{Gyr}. \quad (5)$$

Moore et al. also assumed all subhaloes to be tidally truncated, which for isothermal haloes means $r_s \approx r_h v_s / (3v_h)$. If we do not assume subhaloes to be tidally truncated, the corrected disruption timescale is given by eq. (4). In both cases r_p is set to the softening length ϵ .

The second problem is the relative scaling to subhalo-subhalo heating: Moore et al. state that the rate of energy input via impulse encounters scales as $m_p^2 n_p$, and that therefore the relative importance of subhalo-subhalo encounters versus subhalo-particle encounters can be written as $f m_s / m_p$, where f is the fraction of mass in subhaloes. However, this statement is incorrect, because for the tidal approximation that Moore et al. (1996) adopt, the rate of energy input also depends on the size of the perturber, as

eq. (3) of Moore et al. (1996) clearly shows. So, the rate of energy input actually scales as $m_p^2 n_p / r_p^2$, and the relative importance therefore as $f(m_s/m_p)(r_p/r_s)^2$. This would imply that subhalo-subhalo tidal heating is actually *less* important than particle-subhalo tidal heating, contrary to the claim of Moore et al. (1996). However, the tidal approximation cannot be extrapolated down to $r_p = \epsilon$, as Moore et al. (1996) do. Furthermore, penetrating encounters need to be taken into account as well, so that the energy change is given by a smooth interpolation between penetrating and distant encounters (see van Kampen 2000 for details). For isothermal subhaloes, this means that the energy input scales as $m_p^2 n_p r_p^{-1/2} r_s^{-3/2}$ (van Kampen 2000). Taking this into account, subhalo-subhalo tidal heating is $f(m_s/m_p)(r_p/r_s)^{1/2}$ times faster than particle-subhalo tidal heating. With $f m_s / m_p$ of order ten, this amounts to a factor of a few.

We thus find that the subhalo-subhalo heating timescale is a factor $13(r_s/r_p)^2$ larger than given by Moore et al. (1996), which is more than an order of magnitude. With $m_s/m_p = N_s$, the subhalo-subhalo tidal heating timescale is

$$t_{\text{dis,ss}} \approx \frac{2.4}{f} \frac{r_h}{r_s} \frac{r_h}{v_h}. \quad (6)$$

Typically, r_h/r_s is of order ten, and $f \approx 1/4$, so the disruption timescale is at least 100 embedding halo crossing times, which for cluster galaxy haloes is around 0.3 Gyr, and the disruption timescale is at least 30 Gyr.

However, if one assumes tidal truncation for the subhaloes, as Moore et al. (1996) do, one gets

$$t_{\text{dis,ss}} \approx \frac{7.2}{f} \frac{v_h}{v_s} \frac{r_h}{v_h} = \frac{72}{f} \left(\frac{r_h}{1 \text{ Mpc}} \right) \left(\frac{100 \text{ km s}^{-1}}{v_s} \right) \text{Gyr}. \quad (7)$$

This estimate again is more than an order of magnitude larger than the estimate given by Moore et al. (1996, their eq. 5 at $R_c = r_h$). Tidal truncation of subhaloes clearly reduces the effectiveness of the subhalo-subhalo tidal disruption process by a factor of a few. Still, it remains unclear whether the assumption of tidal truncation is justified, as it takes time for the tidal truncation to take place, if it happens at all. When a halo becomes a subhalo, it will certainly not be truncated straight away.

Note that the timescales as derived above are for unchanging perturbers. However, as the perturbers get disrupted by each other, or by any other means, f will decrease, and the disruption timescale will increase, thus slowing down the subhalo-subhalo tidal heating process. Indeed, Klypin et al. (1999) make the interesting point that even though subhalo-subhalo tidal heating seems like an important effect, in practice many of the subhaloes, especially the smaller ones, get disrupted before they can participate in this process for a long enough time. This also means that at any one time there are not many subhaloes left to tidally heat each other, but there will be an increasing amount of loose N-body particles in the embedding halo to drive two-body heating.

In concluding, subhalo-subhalo tidal heating is clearly not an important physical process within galaxies or galaxy clusters, whether subhaloes are tidally truncated or not.

2.3.3 Dynamical friction

The physical mechanism of dynamical friction leads to the complete destruction of subhaloes by bringing them to the centre of their embedding halo, where they merge with the core region. This process is well-known and extensively discussed in the literature (e.g. Saslaw 1985; Binney & Tremaine 1987; and references therein).

The actual orbit of the subhalo is important, as for the mean tidal field. An estimate for the dynamical friction timescale of a subhalo at r_h on a nearly circular orbit within an isothermal embedding halo is

$$t_{\text{fric}} \approx \frac{1.2}{\ln \Lambda} \frac{r_h^2 v_h}{G m_s} \approx \frac{0.5}{\ln \Lambda} \frac{m_h}{m_s} \frac{r_h}{v_h} \quad (8)$$

(Binney & Tremaine 1987, their eq. 7-26), where we have used the virial theorem for the embedding halo, and $\ln \Lambda$ is the Coulomb logarithm, with $\Lambda \approx m_h/m_s$ for point masses, and

$$\ln \Lambda = \frac{1}{m_s^2} \int_0^{b_{\text{max}}} b^3 \left[\int_b^\infty \frac{m_s(r) dr}{r^2 (r^2 - b^2)^{1/2}} \right]^2 db \quad (9)$$

for extended subhaloes (White 1976). The deceleration by dynamical friction is given by

$$\dot{\mathbf{v}} = -4\pi \ln \Lambda G^2 m_s \rho(<v) \frac{\mathbf{v}}{v^3}, \quad (10)$$

where $\rho(<v)$ is the density of background particles moving slower than the subhalo. For a Maxwellian velocity distribution with dispersion σ this is given by (Binney & Tremaine 1987)

$$\rho(<v) = \rho(\mathbf{r}) \left[\text{erf} \left(\frac{v}{\sqrt{2}\sigma} \right) - \sqrt{\frac{2}{\pi}} \frac{v}{\sigma} e^{-v^2/2\sigma^2} \right]. \quad (11)$$

The most massive subhaloes are destroyed most rapidly, and a maximum mass for a subhalo can be set by setting the dynamical friction timescale to the age of the embedding halo. The dynamical friction timescale is generally *shorter* for eccentric orbits, by a factor of $\eta^{0.53}$ (van den Bosch et al. 1999), where η is the orbital circularity, defined as the dimensionless fraction J/J_c , with J_c the angular momentum of a circular orbit.

For both galaxies and galaxy clusters the mean crossing time is around 0.3 Gyr (with significant scatter), so the dynamical friction timescale will be around $0.04 m_h/m_s$ Gyr (eq. 8), where we have used that $\eta \approx 0.6$ (median value, van den Bosch et al. 1999), and that the Coulomb logarithm $\ln \Lambda$ is of order 3.

If the mass of our Galaxy is $\approx 10^{12} M_\odot$, most subhaloes with $m_h > 5 \times 10^9 M_\odot$ should have been destroyed over the lifetime of our Galaxy. This implies that subhaloes that are observed today have entered the halo only recently. A fraction of the subhaloes with masses of around $10^9 M_\odot$ or less might also have been destroyed, very much depending on their orbits.

For a rich galaxy cluster with mass $10^{15} M_\odot$, galaxy haloes with masses over $10^{13} M_\odot$ are likely to be destroyed within the lifetime of a galaxy cluster. However, as clusters of galaxies are relatively young objects, secondary infall of new galaxy haloes is ongoing, and destroyed haloes can be replaced. This makes it hard to test estimates for the dynamical friction timescale observationally.

Tormen, Diaferio & Syer (1998) tested dynamical friction within galaxy clusters numerically, but unfortunately their simulations contain just 20,000 particles for the embedding halo, which means that many of their subhaloes disrupt through particle-subhalo two-body heating. The simulations of Ghigna et al. (1998) employ a hundred times more particles, and therefore a fair number of subhaloes survive in their simulations. They do not address dynamical friction, but do state that the subhaloes are tracers of their embedding halo. In other words, dynamical friction does not seem to operate in their galaxy cluster simulation. We discuss this further in Section 4.

3 THE DIFFERENCE BETWEEN GALAXY AND CLUSTER SUBHALOES

While it is obvious that subhaloes in galaxy cluster haloes exist (by definition), this is much less obvious for galaxy subhaloes. Our Galaxy contains just two subhaloes with a significant mass (the Magellanic Clouds, with a mass of $\approx 10^{10} M_\odot$ for the LMC), while the remaining subhaloes found are much less massive (eg. Mateo 1998). Clearly, galaxy subhaloes are either destroyed by a physical mechanism, are much darker (i.e. have a much larger mass-to-light ratio) than cluster galaxies, or were never formed in large numbers in the first place, for example if the power spectrum of density fluctuations turns over below or near the galaxy mass-scale. There are five main explanations of this sort, some of which have already been proposed in the literature

(1) *The initial density fluctuation spectrum lacks power on small scales*

This is the most radical explanation, and has major consequences for cosmology. Moore et al. (1999) look at standard CDM only, whereas Klypin et al. (1999a) consider both standard CDM and Λ CDM, the latter being the favoured model at the moment (e.g. Efstathiou 2000b). Thus, the problem could only exist for CDM-like cosmologies. Indeed, a range of models that are distinctly different from CDM-like models have been proposed: Warm Dark Matter (e.g. Bardeen et al. 1986) and self-interacting dark matter (e.g. Spergel & Steinhardt 1999) are two examples, or even a combination of the two (Hannestad & Scherrer 2000). The self-interacting dark matter cosmology is the most tested recently, but seems a mixed blessing (e.g. Moore et al. 2000), as it does not actually solve the galaxy subhalo abundance problem (Yoshida et al. 2000). The Warm Dark Matter cosmology looks the more promising alternative, as it provides a solution to a problem with the angular momentum of disk galaxies as well (Sommer-Larsen & Dolgov 2000).

(2) *Dwarf galaxies are much darker than galaxies*

In hierarchical galaxy formation scenarios there usually is a significant difference in mass-to-light ratio between dwarf galaxies and ‘normal’ galaxies, in the sense that the former are much darker than the latter. This is due to the necessity of strong ‘feedback’, a mechanism in which supernovae reheat a significant fraction of cold gas in the halo to such a temperature that star formation stops for that fraction of gas. In hierarchical galaxy formation some form of feedback is necessary to prevent turning the majority of baryons into stars at high redshift (e.g. Efstathiou 2000a

and references therein), but the strength needed is quite uncertain.

However, even if dwarfs are much darker than galaxies, a large abundance of dark subhaloes within galaxies might still be a problem with respect to the survival of disks (Tóth & Ostriker 1992). Therefore, the dwarf haloes within galaxies should not survive as long and in such high abundances as the simulations seem to indicate.

(3) *Overmerging produces too many small haloes*

Overmerging always plagues N-body haloes and subhaloes consisting of less than a hundred particles or so, as discussed in Section 2.2. Overmerging affects the smallest haloes in the simulations of Klypin et al. (1999b) and Moore et al. (1999), which have particle masses of $4 \times 10^6 h^{-1} M_\odot$ (for the whole simulation volume) and $10^6 h^{-1} M_\odot$ (only within a sphere of twice the virial radius) respectively. Thus, many subhaloes with masses below $10^8 M_\odot$ are destroyed through overmerging, which means that too many haloes with masses over $10^7 M_\odot$ are identified as single (dwarf) galaxy haloes, while they should contain several even smaller (dwarf) galaxies and a population of globular clusters.

(4) *Subhaloes survive in simulations only because of numerical limitations*

The N-body simulation method is an approximate method, so there could be a numerical problem which causes the mismatch with observations. One possible problem is the inability to numerically simulate dynamical friction, even at the highest resolution achieved to date. In other words, there might be a numerical ‘undermerging’ problem: not enough subhaloes are destroyed within galaxy haloes in the simulation. We explore this possibility in Section 4.

(5) *Galaxy clusters contain more subhaloes than galaxies due to the timing of hierarchical structure formation*

The timing of halo formation and merging within the hierarchical formation of structure in the Universe can cause significant differences in the destruction rate of subhaloes in embedding haloes of different mass, but also differences in the rate at which destroyed subhaloes are replaced by newly accreted ones. Whatever process causes subhalo destruction, any such process is given more time to operate within galaxy haloes, as these form earlier than galaxy cluster haloes. Furthermore, galaxy clusters clearly show active secondary infall, whereas this is not obvious at all for galaxies. Thus, even if destruction is as effective in clusters as in galaxies, one still sees more subhaloes in clusters because destroyed subhaloes are being replaced, whereas galaxy subhaloes are not.

4 DYNAMICAL FRICTION REVISITED

In the derivation of the dynamical friction timescale (e.g. Binney & Tremaine 1987) it is assumed that the subhalo moves through a homogeneous background, or at least through a sea of a large number of small particles. The highest resolution simulations (e.g. Moore et al. 1999 and Klypin et al. 1999a) have just over 10^6 particles. Therefore, it is likely that the numerical resolution is not good enough to properly sample the gravitational wake that provides the effective drag force acting on a subhalo moving through an

embedding halo (e.g. Mulder 1983), which contains an almost infinite abundance of dark matter particles. Zaritsky and White (1988) already concluded that simulations of dynamical friction sensitively depend on subtle details of the simulation technique, so resolution is likely to be an important factor.

The possibility of ‘undermerging’, due to the inability to properly simulate dynamical friction, can be tested using simulations of the same halo-subhalo system at very different resolutions, i.e. particle numbers. Previously, such tests have only been performed for a small range in particle number (e.g. Cora, Muzzio & Vergne 1997; van den Bosch et al. 1999). Here, we discuss series of simulations of equilibrium Plummer models, where for each series we ran four simulations, with 10^3 , 10^4 , 10^5 , and 10^6 particles for the embedding halo. The 10^6 particle simulations are the largest to date performed for this purpose.

4.1 Global and local dynamical friction

In the original derivation of the dynamical friction formula by Chandrasekhar (1943) the object under study moves through an infinite, uniform medium, and dynamical friction is solely driven by the density response. However, a subhalo orbiting within an embedding halo will also tidally deform that halo, and such global distortions exert a torque on the subhalo, thus changing its angular momentum. We call this effect *global* dynamical friction, to contrast it with the *local* dynamical friction driven by the gravitational wake (density response) of the subhalo. There has been much debate in the literature over whether dynamical friction is predominantly local or global (e.g. Zaritsky & White 1988; Weinberg 1989; Cora et al. 1997; Colpi et al. 1999). Most authors conclude that it is local, on the basis that timescales measured in simulations are in fair agreement with Chandrasekhar’s formula, even though that was not derived for a halo-subhalo configuration. However, these tests are generally for a *single* subhalo on a circular orbit, which is optimal for global dynamical friction. Thus, in such simulations the wake might not be modelled properly at all, while the subhalo still decays due to global tidal distortions, which is not incorporated in the formalism of Chandrasekhar (1943).

In reality, *many* subhaloes populate the embedding halo at any one time, on a variety of orbits. This means that global distortions induced by each of these subhaloes add up to form a stochastic net distortion pattern. Thus, the angular momentum changes stochastically as well, and the cumulative effect on the subhalo is zero, i.e. global dynamical friction becomes insignificant. Therefore, subhaloes can thus only decay through local dynamical friction, but only if the wake is properly modelled in the N-body simulation.

4.2 Structure of the wake

An important issue addressed in this paper is how well dynamical friction can be modelled using N-body simulation techniques. In order to assess this, we need to establish the volume and shape of the *effective* gravitational wake that generates the drag force, and thus the actual number of N-body particles that are available to model this wake. For this purpose we employ the formalism of Danby & Bray (1967),

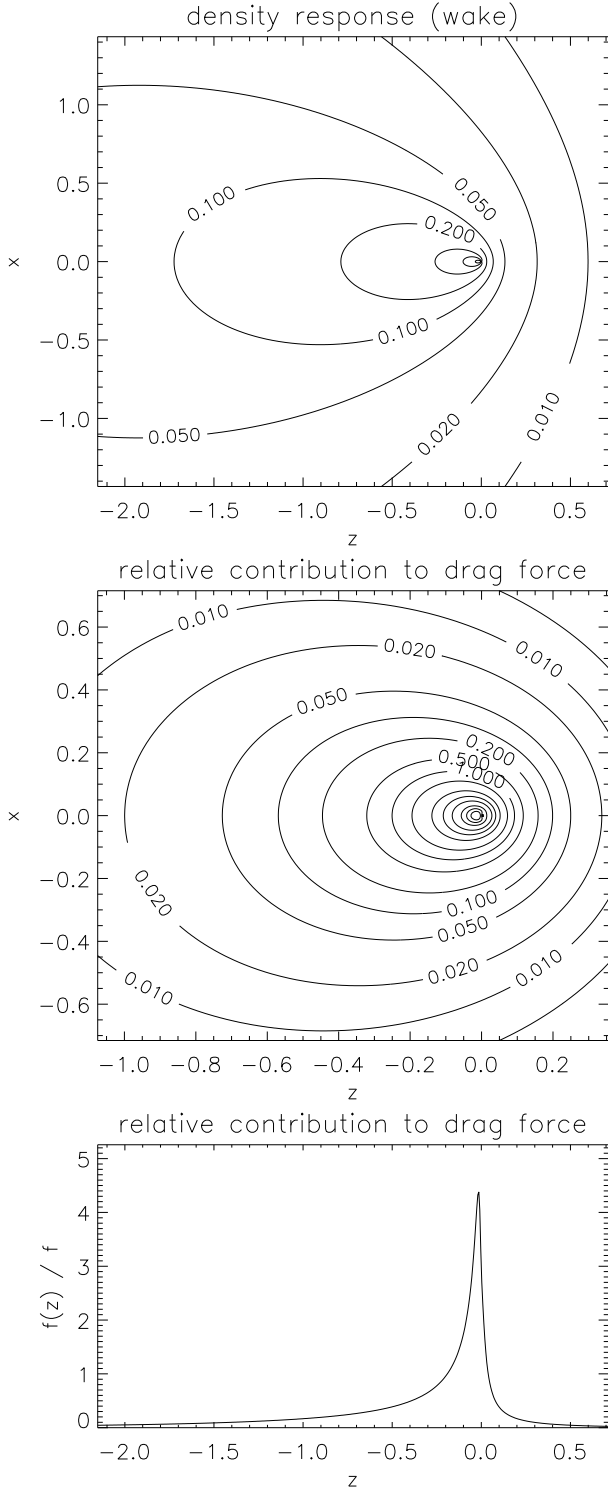


Figure 1a. The top panel shows the density response, or gravitational wake), that drives dynamical friction for a compact subhalo ($R_h/R_s = 6$). The middle panel shows the relative contribution to the total drag force on the subhalo as a function of position. The bottom panel shows the same, but as a function of z only.

which allows one to calculate the density response of any extended subhalo moving through a uniform background density field.

The difference between compact and very extended subhaloes is shown in Figs. 1a and 1b, in which the density re-

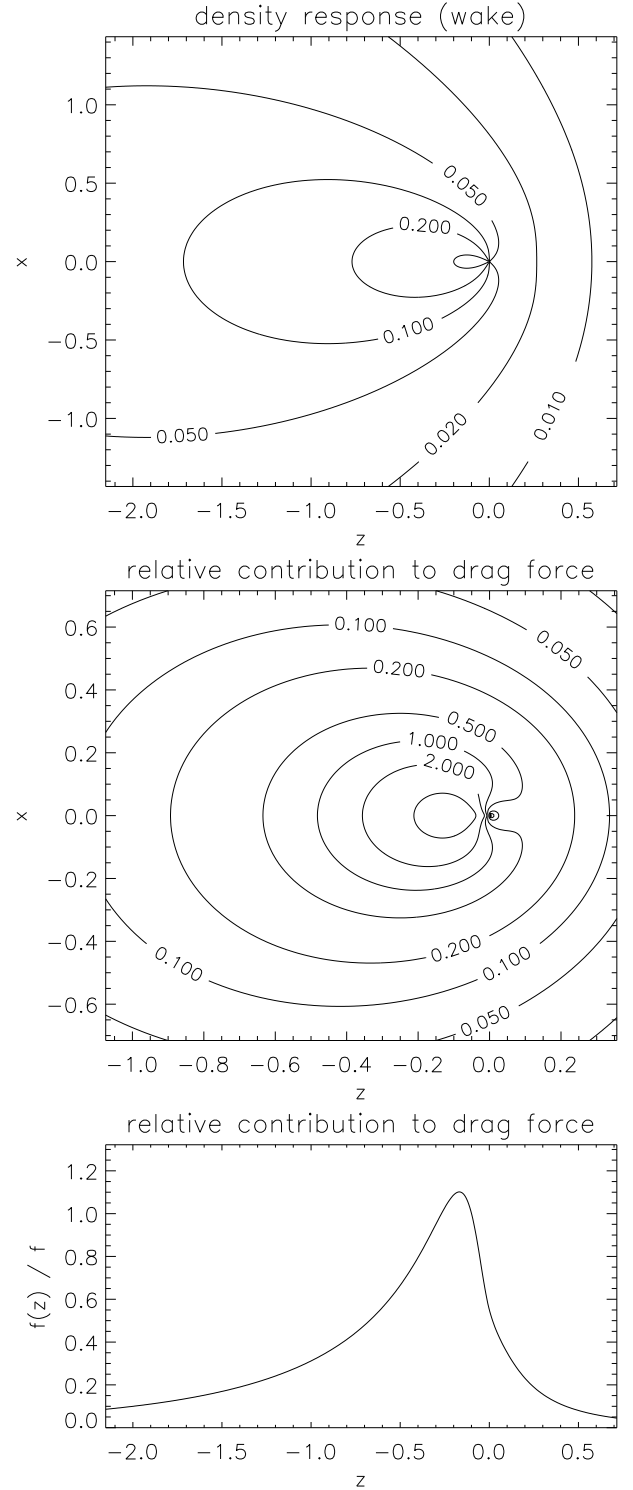


Figure 1b. Same as Fig. 1a, but for an extended subhalo, with $R_h/R_s = 60$. The wake is clearly more extended than for the compact subhalo, with a peak which has a size on the order of the size of the subhalo. This is also true for the compact subhalo (See Fig. 1a).

sponse $\rho_{\text{res}}(x, y, z)$ is plotted in the $x - z$ plane, with the subhalo moving along the z -axis (top panels). In order to establish the relative importance of each spatial position towards the cumulative dynamical friction force, first note the cylindrical symmetry of the problem. This means that we

only need to consider the drag force along a circle at (R, z) , with $R^2 = x^2 + y^2$ being the cylindrical coordinate defined as the distance to the z -axis. The contribution to the total drag force on an extended spherical subhalo at $(0, 0)$ from the density response at (R, z) is $\rho_{\text{res}}(R, z)M_s(< r)/r^2$, with $r^2 = R^2 + z^2$. For Plummer subhaloes this is equal to $\rho_{\text{res}}(R, z)M_s r / (R_s^2 + r^2)^{3/2}$. For the two specific subhaloes considered this quantity is shown in the corresponding middle panels of Figs. 1a and 1b, again in the (x, z) -plane, but zoomed in by a factor of two with respect to the top panels. Integrating over R , we obtain the relative contribution to the drag force as a function of z only, which is shown in the lower panels of Figs. 1a and 1b.

What Figs. 1a and 1b demonstrate is that the contribution to the drag force acting on a compact subhalo comes mostly from a compact region just behind the subhalo, whereas for more extended subhaloes this region is more extended as well. It is clearly much harder to form a compact wake within an N-body simulation with limited resolution at the subhalo scale. The figures also demonstrate a point already made by Mulder (1983), which is that the density response contours are identical well away from the subhalo, with the only difference being their amplitude. Thus, if the narrow peak of the wake behind the compact satellite is not formed due to a lack of particles, the density response of both the compact and extended subhaloes will look identical with a much smaller difference in amplitude than predicted by Chandrasekhar's formalism.

4.3 Single subhalo simulations

In the first series of test models we introduce at the half mass radius a single, rigid subhalo with a mass of 1 per cent of the mass of the embedding halo. Its orbit is mildly eccentric, with orbital circularity $\eta = 0.73$ (see Section 2.3.3 for the definition of η). This series represent the 'classical' dynamical friction test, i.e. a single subhalo decaying towards the centre of a halo. Both halo and subhalo are modelled by a Plummer density profile, with characteristic radii R_h and R_s respectively. For this configuration the Coulomb logarithm is given by

$$\ln \Lambda = \frac{1}{2} \left[\ln(1 + R_h^2/R_s^2) - \frac{R_h^2/R_s^2}{1 + R_h^2/R_s^2} \right]. \quad (12)$$

(Cora et al. 1997). For $(R_h/R_s) > 4$ this relation is well approximated by $\ln \Lambda = \ln(R_h/R_s) - 0.5$. We set $R_h/R_s = 60$, which implies $\ln \Lambda = 3.6$. This would lead to a dynamical friction time of 12 embedding halo crossing times for an isothermal sphere (eq. 8), but for a Plummer model the subhalo decays in 3 to 5 embedding halo crossing times. The main reason for this faster decay is that the subhalo starts at the half-mass radius r_h , which is close to R_h for the Plummer profile: $r_h \approx 1.3R_h$. Thus, it is already near the core of almost constant density, which never happens for the core-less isothermal profile. The Plummer density profile was chosen for the test runs because the large core assures that the system behaves well numerically. Also, the particle density will be larger for a larger volume of the simulation than for an isothermal profile, so that the number of particles inside the wake will also be larger. This does mean that if it is not possible to properly simulate dynamical friction for a Plummer model, it is certainly not possible for an isothermal or other

core-less halo.

The dynamical friction time for an isothermal halo is well-defined, being by the angular momentum evolution $L(t) \sim -t^{1/2}$ (e.g. Binney & Tremaine 1987, from their eq. 7-25). However, this is not the case for the Plummer halo, for which $L(t)$ evolves fast near R_h , but slower near its centre. An analytical expression for $L(t)$ for a Plummer halo does not exist, so $L(t)$ was solved numerically, using two quite different methods. For the first method the calculation of Binney & Tremaine (1987) for the isothermal halo is adapted for a Plummer halo, but the more complicated equation of motion is solved numerically. The second method is even more numerical, as a special N-body code is used to solve the two-body halo-subhalo system, in which the dynamical friction deceleration given by eq. (10) is explicitly added to the equations of motion coded in the N-body simulation.

We show $r(t)$ and $L(t)$ of the subhalo as a function of numerical resolution in the left-hand panels of Fig. 2 (solid lines), where increasing thickness of the lines indicate increasing resolution. The two theoretical solutions for $L(t)$ for the subhalo are shown as a dashed line (numerical solution to the Binney & Tremaine formalism) and a dotted line (the special N-body code). The dot-dashed line shows the theoretical evolution of $L(t)$ for a point mass subhalo, which represent the fastest decay possible for a subhalo of this mass and initial orbit, i.e. $\ln \Lambda = \ln(m_h/m_s) = 4.6$. At all resolutions we see the orbit of the subhalo decay, but this happens increasingly faster for simulations with increasing resolution. More important, however, is the observation that the $L(t)$ curves converge towards the theoretical curve, but do *not* match it even for 10^6 particles. Thus, the subhalo needs twice as long to decay even in the highest resolution simulation. The most obvious explanation is that the gravitational wake that drives dynamical friction is not properly modelled due to insufficient resolution.

In order to visualize this, we look at the density response of the embedding halo in three of the runs from the first series (for 10^4 , 10^5 , and 10^6 particles). First, the small-scale density was calculated using a Gaussian filter of 30 kpc, where the subhalo particle was excluded. Then, the Plummer density law was fitted to the particles of embedding halo, again excluding the subhalo. The resulting *response density* i.e. the difference of the simulated density and the smooth Plummer law, is shown in Fig. 3a. The particles in a thin slice within the plane of the subhalo's orbit are plotted, with a colour coded level indicating the response density. The position and velocity of the subhalo after two embedding halo crossing times, are indicated by a large black dot and a thick line-segment respectively. Its orbit is shown as a thin solid line. The wake can clearly be seen in the bottom panels, but is absent in the top panels.

However, before pointing at insufficient resolution as the cause for the slower than expected decay of subhaloes in N-body haloes, we should look at a configuration where resolution should be less of a concern. For this purpose we ran a second series of simulations, completely identical to the first one, in which the subhalo is taken to be 10 times larger in extent, but with the same mass and initial orbit. Setting $R_h/R_s = 6$, we get $\ln \Lambda = 1.3$, which is also used to calculate (numerically) two new theoretical predictions for $L(t)$. The results are plotted in the right-hand panels of Fig. 2, for the same range in particle number as the first run.

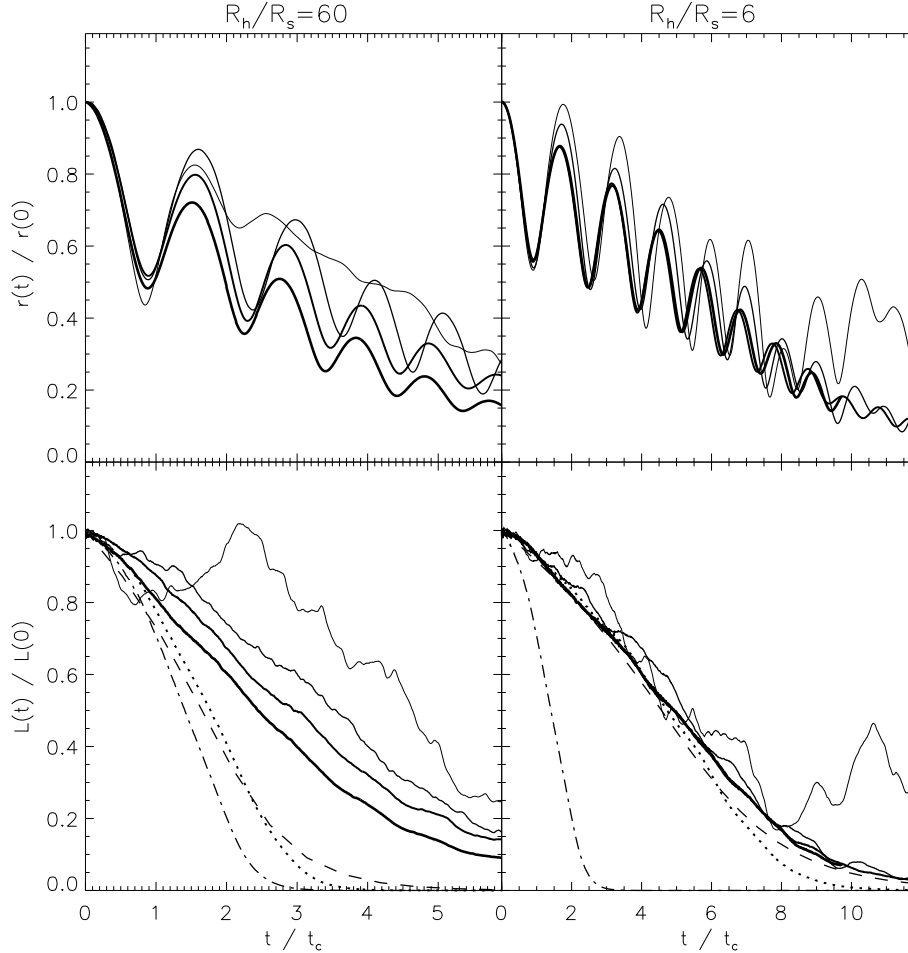


Figure 2. Time evolution of the radius and angular momentum of the slightly eccentric orbit ($\eta = 0.76$, see main text) of a subhalo initially at the half-mass radius of its embedding halo. In each panel the four solid lines represent the N-body simulations, with the thickness of the line increasing with the number of particles, being 10^3 , 10^4 , 10^5 , and 10^6 particles (i.e. the thickest solid line represents the highest resolution simulation). The dotted and dashed line are theoretical predictions, calculated in two different ways (see text), while the dot-dashed line gives the theoretical prediction for a point mass, representing the fastest decay by dynamical friction that is possible.

At all resolutions, we see the subhalo spiralling towards the centre at roughly the same rate, except for the 10^3 particle run, which clearly shows two-body interactions to be important all the way. The decay is slower than for the more compact subhalo modelled in the first run, as it should be, but most interestingly, it is a fair match to the theoretical curve. Furthermore, a wake, plotted in Fig. 3b, is visible not only for the 10^6 particle run, but also for the 10^5 particle simulation, and maybe even for the 10^4 particle run.

Thus, for a subhalo this size, dynamical friction seems to be modelled properly using as little as 10^4 particles for the embedding halo. However, it is still not certain whether the gravitational wake is actually modelled properly, because global dynamical friction could also drive part or even most of the decay, and the wakes visible in Figs. 3a and 3b might well be weaker than predicted. If this is the case, the match with Chandrasekhar’s prediction is coincidental.

Besides the gravitational wake, Figs. 3a and 3b also show the global distortion induced by the subhalo. What is important is that the distortions can be seen for *all* resolution. This means that global dynamical friction is clearly an

active process in an N-body simulation of a halo with a single subhalo, irrespective of numerical resolution. It is quite possible that global dynamical friction drives most of the decay of the orbit of this single subhalo. It is thus essential to see what happens for multiple subhaloes.

4.4 Multiple subhaloes simulations

A shortcoming of the ‘classical’ dynamical friction test is that just a single subhalo is considered, which is not realistic for hierarchical structure formation scenarios. It is also not a proper test for Chandrasekhar’s dynamical friction formula, as global tidal distortions (as visible in Figs. 3a and 3b) drive orbital decay as well, which is not likely if many subhaloes orbit the same halo (as discussed in Section 4.1). This leads us to perform a third series of simulations, in which the first subhalo is taken to be identical to the subhalo of the first series, but twenty more subhaloes are added, on random orbits.

Each of the subhaloes can only decay through local dynamical friction, with a timescale given by the Chan-

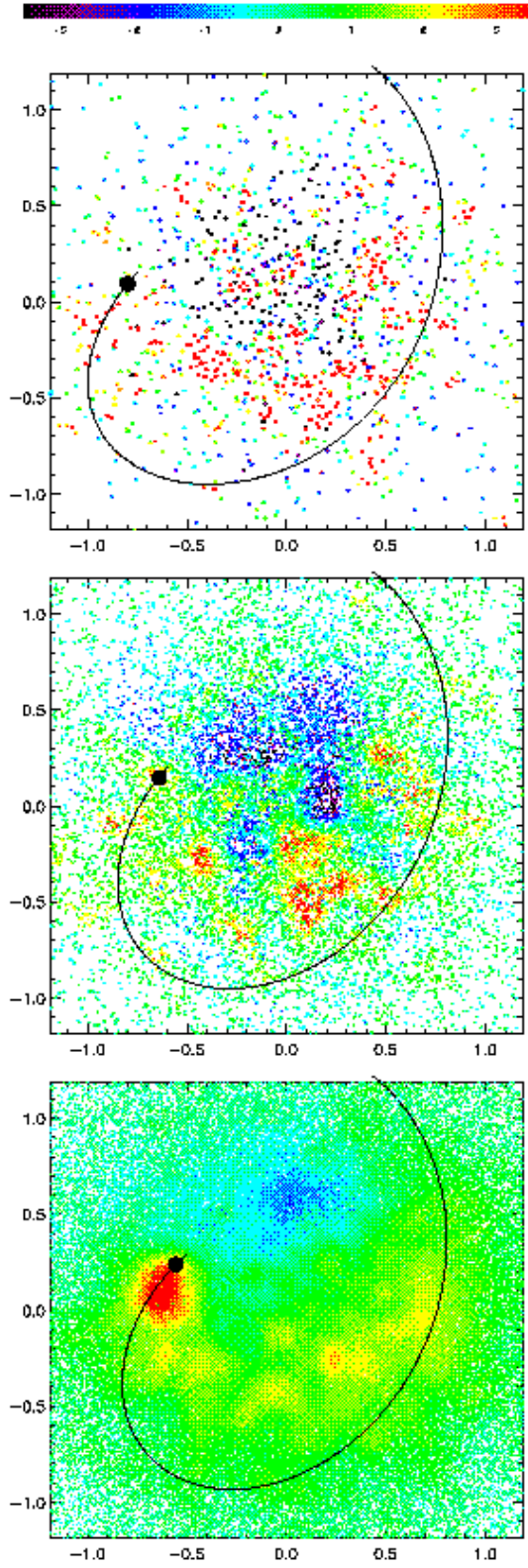


Figure 3a. The density response due to a compact subhalo for three different numerical resolutions: 10^4 (top panel), 10^5 (middle panel), and 10^6 (bottom panel) particles for the parent halo.

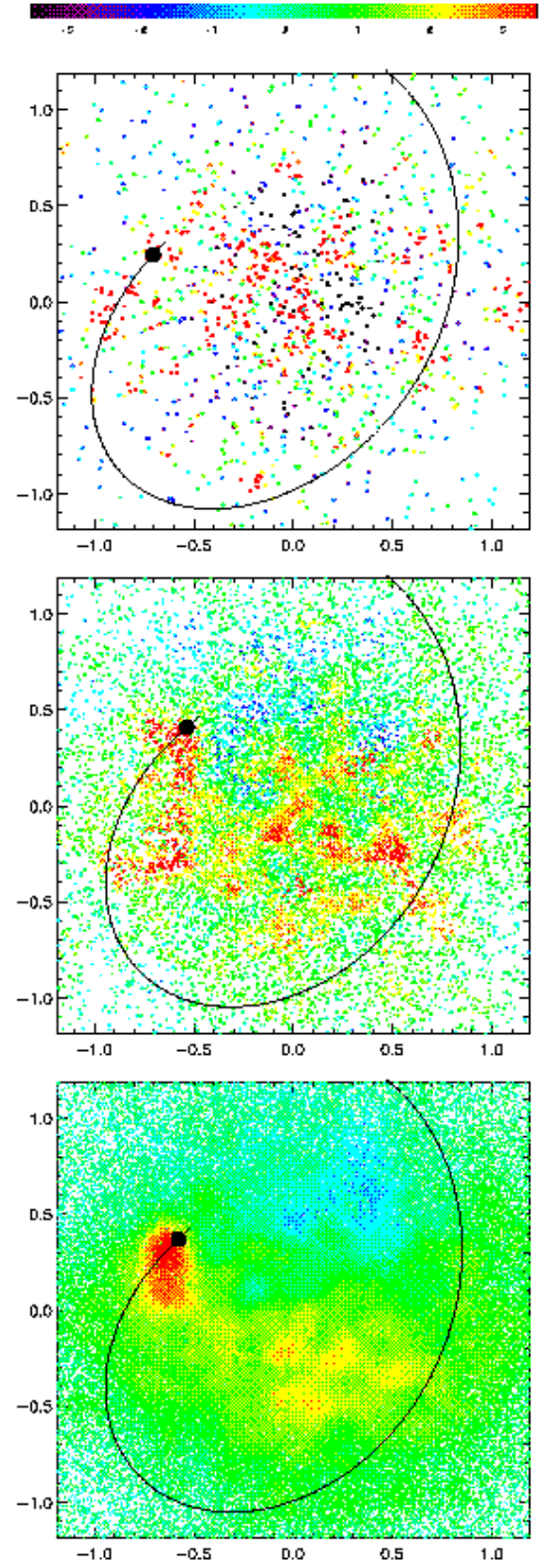


Figure 3b. As Fig. 3a, but for an extended subhalo.

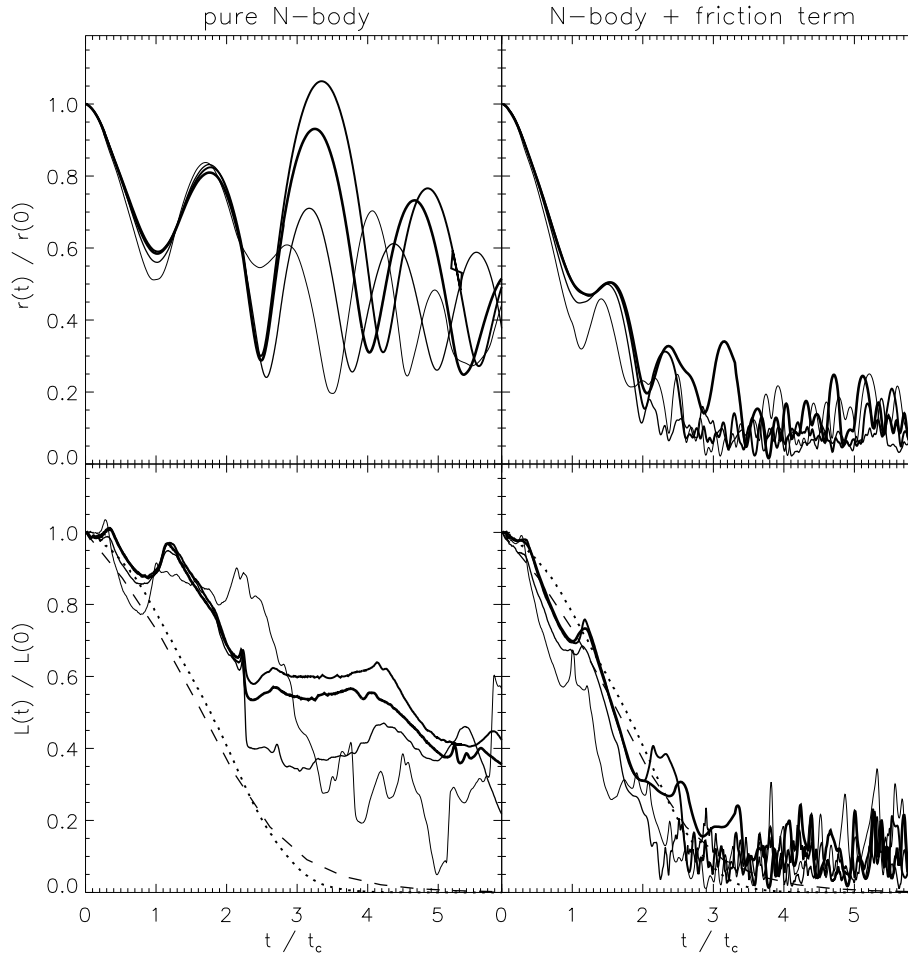


Figure 4. Same as Fig. 2, for the $R_h/R_s = 60$ subhalo, which now shares its parent halo with 20 more subhaloes of the same type. The left-hand panels show the result of re-running the same simulation that produced the results shown in the left-hand panels of Fig. 2. The right-hand panels show the result of explicitly adding to the equations of motion the local dynamical friction force according to Chandrasekhar (1943).

Chandrasekhar formalism (eq. 8), because global distortions from multiple subhaloes form a net stochastic force which both accelerates and decelerates each subhalo, without the net effect of decay. Even more stochasticity comes from the sum of forces from all subhaloes and their wakes. These forces should average out over time, so each subhalo decays only under the influence of their own wake, which will be the closest overdensity at most times.

The evolution of radius and angular momentum for the original subhalo are plotted in the left-hand panels of Fig. 4. Their evolution clearly shows the influence of the stochastic forces discussed above. The orbit decays only some of the time, and less rapidly. Also, the subhalo does not reach the centre of its parent halo after six crossing times, as it did in the single subhalo simulation (see Fig. 2). Some of the added subhaloes do not decay at all, even though they start at roughly the same radius. This is shown in the left-hand panels of Fig. 5, which again shows the evolution of radius and angular momentum, but for one of the added subhaloes.

If the density response were properly modelled, local dynamical friction would bring the subhaloes towards the centre of their parent halo within a few crossing times. In order to show this, the friction force is explicitly added to

the equations of motion in the N-body code. The local density is calculated using Gaussian smoothing of the particle distribution, and the velocity distribution is assumed to be Maxwellian, which is true for the test models considered here, but not for general cosmological mass distributions. The results of re-running the simulations with the local friction term added are shown in the right-hand panels of Figs. 4 and 5, for the same two subhaloes shown in the left-hand panels of these figures.

Not surprisingly, the two subhaloes, and indeed all other subhaloes, decay at the predicted rate. The point of this exercise is to show that if dynamical friction were properly modelled, it is very effective in destroying subhaloes. However, unless a drag force is explicitly added, even a halo of 10^6 particles is not capable of modelling local dynamical friction self-consistently. Dynamical friction is only effective in numerical simulations of a single subhalo system, where global dynamical friction drives the orbital decay.

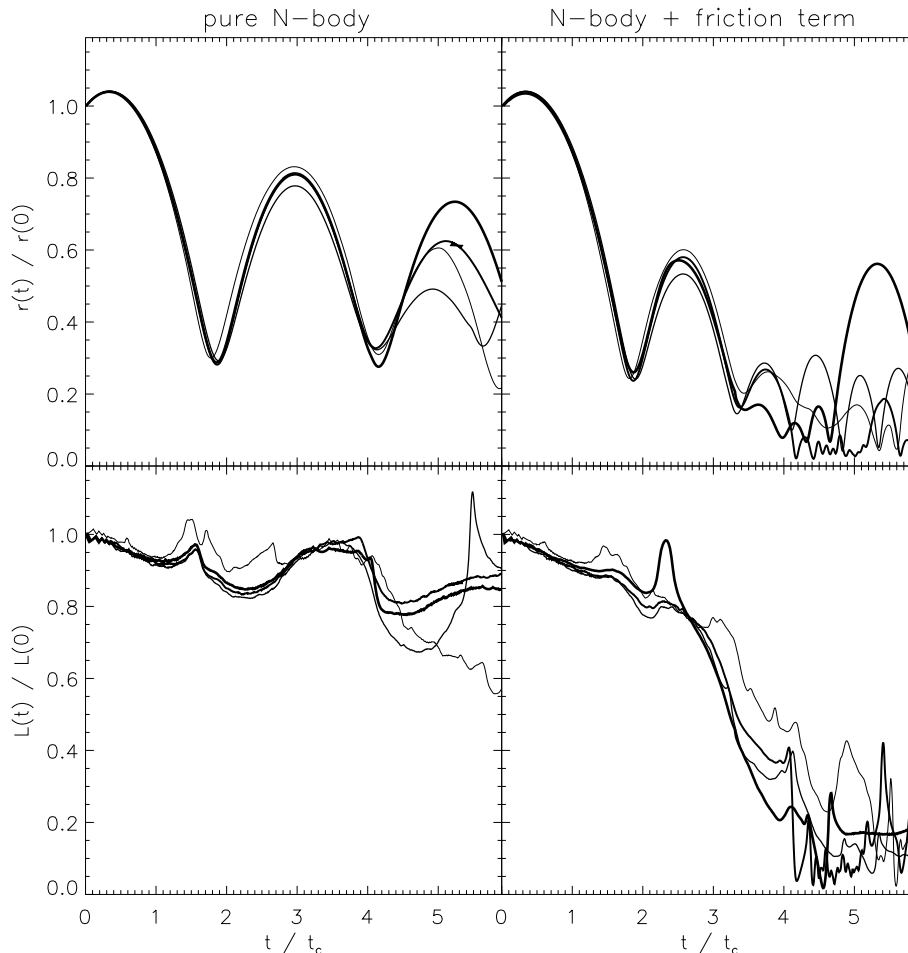


Figure 5. Same as Fig. 4, but for another subhalo (one of the twenty that were added to the configuration used to produce Fig. 2).

4.5 What is needed to properly model dynamical friction ?

How many particles are required to properly model the gravitational wake that drives (local) dynamical friction ? From the test above it seems that the answer is at least 10^8 particles for single subhalo systems, but probably a lot more, as the multiple subhalo simulations demonstrate. The main problem is the lack of particles near the subhalo to form a strong and sustainable wake, especially away from the centre of the embedding halo where the N-body particle density is low. The extent of the wake is determined by the extent of the subhalo and its velocity with respect to the rest-frame of its parent halo, in the sense that the wake is more extended with a lower maximum response density for a more extended and/or slower subhalo (Mulder 1983). Thus, for the more compact subhalo of the first series, the wake is more linear, aligned along the orbit of the subhalo. This wake consists of fewer particles, which responded stronger to the compact subhalo than to the extended one, and the compact subhalo wake is therefore more fragile numerically. The problem is worse in the outskirts of the embedding halo, where the N-body particle density is lowest and the response density peak therefore more sparsely sampled, and for large subhalo velocities, especially for a subhalo that just entered a halo. In the latter case the wake is quite narrow (see Fig.

2b of Mulder 1983), and again hard to sample using the available particles from the embedding halo.

Another numerical problem is that two-body interactions can disrupt a wake, just like small subhaloes are disrupted by two-body interactions (see Section 2.2). Can we use eq. (2) to estimate a wake disruption timescale ? This seems unlikely, as the wake is not a simple collapsed structure. An N-body particle that is part of a wake only remains so for some time. During this time, the only two-body interaction such a particle should have is with the subhalo, and not with other particles in the wake. Thus, the number of particles in and around the wake should be large enough to prevent this. The simulations as performed show this: for the more extended subhalo in the second series of test simulations the volume of the wake is fairly wide, and thus the number of particles is sufficient even for the $N_h = 10^4$ run. But for the compact halo, the wake has a compact density response maximum, which seems easy to disrupt by two-body effects.

Thus, if far too many particles are required to simulate dynamical friction self-consistently, the solution is to explicitly add the drag force to the equations of motion, as was done for the fourth series of test simulations presented above. However, this was easy to implement for the Plummer halo, as its properties could be coded directly and the velocity distribution function is known, but this will be much

harder for cosmological N-body simulations in which haloes can have any profile and typically are not smooth and relaxed, and subhaloes are not single particles. It will therefore require some ingenuity to explicitly include the dynamical friction force in a cosmological N-body code.

5 TIMING

In hierarchical clustering, haloes grow through merging with other haloes. This growth is not continuous, but occurs in distinguishable merger events, with relatively quiet periods in between. During these periods substructure, including subhaloes, can be destroyed by the physical processes described in Section 2.3, and in simulations also by the numerical processes described in Section 2.2. When comparing the survival of subhaloes in galaxies and in clusters, the epoch and duration of these quiet intervals between merger events surely must play an important rôle. In order to investigate this we first estimate the mean formation epoch of a halo of a given mass M (or corresponding circular velocity v_c).

5.1 Halo formation epoch

The Press-Schechter formalism gives a good description of the collapse of haloes, and therefore of their formation rate. For the special case of an Einstein-de Sitter universe the halo formation rate is given by

$$\frac{dn(M)}{dt} \sim (1+z)^{\frac{7}{2}} e^{-\delta_c^2(1+z)^2/(2\sigma^2(M))} \quad (13)$$

(Percival & Miller 1999), where $n(M)$ is the number density of haloes, $\delta_c \approx 1.67$ is the critical overdensity for collapse, and $\sigma(M)$ is the variance of the density field filtered with a sharp k -space filter corresponding to the mass-scale M . The peak formation epoch is given by

$$z_{\text{peak}}(M) = \left(\frac{7\sigma^2(M)}{2\delta_c^2} - 1 \right)^{\frac{1}{2}}. \quad (14)$$

The spherical collapse model can be used to assign a circular velocity to a halo of mass M forming at redshift z :

$$v_c = \left(\frac{M}{2.35 \times 10^5 h^{-1} M_\odot} \right)^{\frac{1}{3}} (1+z)^{\frac{1}{2}} \text{ kms}^{-1} \quad (15)$$

(e.g. White 1996). Instead of $z_{\text{peak}}(M)$, we plot the corresponding look-back time $t_{1,\text{peak}}$ (with $t_1 = t_0 - t$, and t_0 the age of the Universe) as a function of v_c in the top panel of Fig. 6, for the standard CDM spectrum normalized to $\sigma_8 = 0.67$.

The *mean* formation redshift is obtained by integrating over time up to but not beyond the present epoch t_0 :

$$\langle z_{\text{form}}(M) \rangle = \left[\int_0^{t_0} n(M) dt \right] / \left[\int_0^{t_0} n(M) dt \right]. \quad (16)$$

Again, the corresponding look-back time $t_{1,\text{form}}(v_c)$ is plotted in the middle panel of Fig. 6. For convenience, $t_{1,\text{form}}(M)$ is shown in the bottom panel of Fig. 6.

5.2 Available time for subhalo disruption

Having established when haloes form through merging of small haloes, one can then estimate how much time is available to the new halo to destroy its subhaloes. From the mean

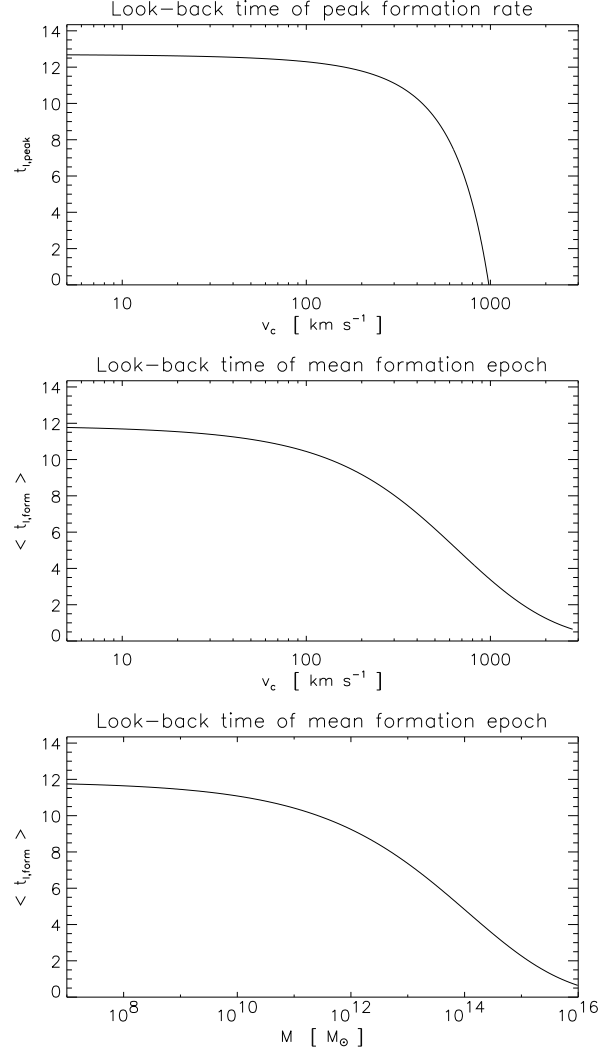


Figure 6. The top panel shows the look-back time of the *peak* formation rate of a halo with a given circular velocity. The middle and bottom panels display the same for the *mean* formation epoch, as a function of halo circular velocity and halo mass respectively.

formation look-back times shown in Fig. 6 it is straightforward to see that dwarf galaxies with $v_c = 10 - 20$ km s⁻¹ form 11.5 Gyr ago, galaxies with $v_c = 100 - 200$ km s⁻¹ form 9 - 10.5 Gyr ago, whereas galaxy clusters with $v_c = 1000 - 2000$ km s⁻¹ form on average 1-3 Gyr ago. This means that dwarfs falling into galaxies had, on average, about *four times* more time to be disrupted than galaxies falling into clusters.

5.3 Subhalo replacement rates

Even if subhaloes are efficiently destroyed by their embedding halo, be it a galaxy or a galaxy cluster, new subhaloes can fall in and replace the destroyed ones. This is certainly happening for galaxy clusters, for which the peak formation epoch is right about now (see top panel of Fig. 6). However, roughly half the galaxies formed about 9 Gyr ago, and very few are forming at the present epoch. Thus, continued

growth by secondary infall, as seen for galaxy clusters, is almost absent. Thus, even if the destruction rate for subhaloes in galaxies and clusters are exactly the same, cluster galaxies are being replaced in fair numbers, while galaxy subhaloes are not.

5.4 Dynamical friction during hierarchical structure formation

An important factor in the efficiency of dynamical friction is the mass ratio of the embedding halo to its subhalo, m_h/m_s . Taken at face value, this means that a $10^9 M_\odot$ dwarf within a $10^{12} M_\odot$ isothermal galaxy decays in of order 40 Gyr (see Section 2.3.3). However, such a dwarf is likely first spend some time in a smaller galaxy, before ending up in the $10^{12} M_\odot$ galaxy. For example, assume that through hierarchical merging it spends 1 Gyr in a $10^{10} M_\odot$ galaxy, then 2 Gyr in a $10^{11} M_\odot$ galaxy, and finally 6 Gyr in a $10^{12} M_\odot$ galaxy. The dynamical friction times are then, respectively 0.4, 4, and 40 Gyr. Thus, this example subhalo will already be destroyed by the $10^{10} M_\odot$ galaxy before the latter grows to a $10^{11} M_\odot$ galaxy. Here we have not taken into account that the crossing time of the $10^{10} M_\odot$ galaxy at look-back time $t_1 = 9$ Gyr is typically smaller than for the final $10^{12} M_\odot$ galaxy, and that its mean density is larger than for a $10^{10} M_\odot$ galaxy that formed recently, which will speed up dynamical friction.

This example illustrates that the very nature of hierarchical clustering within an expanding Universe implies that dynamical friction is much more efficient when taking into account the growth of the embedding halo and the expansion of the Universe (i.e. densities are higher at higher redshifts).

6 SUMMARY, DISCUSSION AND CONCLUSIONS

This paper considered the various numerical and physical processes driving the disruption of subhaloes, with the specific aim to find out whether subhaloes can survive within galaxies, as they do in galaxy clusters. This was prompted by the results of Klypin et al. (1999b) and Moore et al. (1999), who found a large discrepancy between simulations and observations with regard to the abundance of galaxy subhaloes.

Two-body heating is the most efficient of the numerical processes, but only effects small subhaloes, i.e. of order 100 particles or less. Thus, given enough particles, the overmerging problem is resolved, and only physical processes can operate on subhaloes. But do they? In Section 3 it was shown that subhalo-subhalo heating is not an important process (contrary to the claim of Moore et al. 1996), while the mean tidal field of an embedding halo only tidally limits subhaloes, but generally does not destroy them completely. A surprising finding of this paper is that the physical process capable of completely destroying subhaloes, dynamical friction, is not properly modelled by the N-body simulation technique. It was found that in order to properly model the gravitational wake that produces the dynamical friction drag force, one needs a much higher resolution than can be achieved at present.

For single subhalo systems, the problem does not manifest itself because part of the orbital decay is due to global distortions induced in the embedding halo by the orbiting

subhalo. This ‘global’ dynamical friction adds to the ‘local’ dynamical friction produced by the gravitational wake. Test simulations in which the resolution was increased from 10^3 to 10^6 particles (for the embedding halo) showed that the subhalo angular momentum decreased increasingly faster with particle number, but only in a logarithmic fashion, and without any sign of convergence to the expected rate. The problem does show for multiple subhalo systems, in which global dynamical friction does not operate. Thus, only local dynamical friction acts on each of the subhaloes, but even at the highest resolution presently feasible, the wake is not nearly as strong as it should be, and orbital decay is far too slow. Still, increasing the number of simulation particles results in faster decay, so there exists a (very high) number of particles for which the gravitational wake is properly simulated. As this is not the case for current simulations, too few subhaloes are destroyed, and due to the insufficient resolution there is in effect an undermerging problem.

All this means that there are five possible causes for the galaxy subhalo problem:

- (1) the initial density fluctuation spectrum cuts off near the dwarf galaxy scale
- (2) dwarf galaxies are much darker than galaxies due to strong feedback
- (3) overmerging produces too many dwarf galaxy haloes (except within more massive haloes, of course) in simulations with particle masses of order $10^6 M_\odot$
- (4) dynamical friction is not properly simulated even at the highest numerical resolution achieved to date (undermerging)
- (5) due to the timing of hierarchical formation and merging of haloes, galaxy subhaloes are more easily destroyed than cluster subhaloes

In order to solve the galaxy subhalo problem, at least one or more needs to be true. The simplest but most radical solution is for cause (1) to be true in the extreme, i.e. there is no power on small scales so that very few dwarfs galaxies actually form during a Hubble time. Another simple solution is to assume that a significant feedback mechanism operates in dwarf galaxies, so that mass-to-light variations alone can explain the deficiency in observed dwarfs. But then there remains a large abundance of dark dwarf galaxy *subhaloes*, which pose a problem to the survival of a stellar disk. Clearly, it is perfectly acceptable to have plenty of dark dwarfs in the field, but only if they are efficiently destroyed after becoming part of a (bigger) galaxy halo.

This plausible picture is not supported by the simulations of Moore et al. (1999) and Klypin et al. (1999b). However, the results of the test simulations presented in this paper suggest that numerical shortcomings provide the answer, with the main culprits being undermerging, which is the inability of N-body simulations to properly simulate the gravitational wake that drives dynamical friction, and overmerging of the smallest haloes, due to two-body interactions. The consequence of undermerging is that subhaloes are not destroyed in sufficient numbers, while overmerging overproduces them. This produces an artificially high abundance of subhaloes only if overmerging operates on a smaller mass-scale than undermerging, which is the case for simulations with of order $10^6 - 10^8$ particles. This includes the simulations of Moore et al. (1999) and Klypin et al. (1999b).

The numerical problems are especially bothersome dur-

ing the early stages of hierarchical structure formation, where both haloes and subhaloes are modelled by relatively few particles. Galaxy haloes are, on average, four times older than galaxy cluster haloes, and without much ongoing secondary infall. Subhaloes that are destroyed are not all replaced; in this picture, the Magellanic Clouds are relatively new to our Galaxy, and will be destroyed within a few Gyr (Tremaine 1976).

In concluding, it is likely that several of the five causes mentioned above conjure to completely solve the apparent galaxy subhalo problem. The main problem is that dynamical friction is not properly simulated yet, even in the highest resolution simulations to date, due to numerical limitations which, paradoxically, result in an 'undermerging' problem. This is made worse by the timing of halo formation and merging in hierarchical structure formation, which favours destruction of subhaloes in galaxies over subhalo destruction in galaxy clusters. Finally, recent galaxy formation models predict a larger mass-to-light ratio for galaxy subhaloes than for galaxy cluster subhaloes. The net effect of these three causes is that galaxies have a relatively low abundance of subhaloes, i.e. dwarfs, while at the same time a large number of field dwarf galaxies can exist which are dark enough to be missed observationally.

ACKNOWLEDGEMENTS

Many thanks to Frank van den Bosch, Ben Moore, John Peacock, and Will Percival for fruitful discussions and comments.

REFERENCES

- Allan A.J., Richstone D.O., 1988, *ApJ*, 325, 583
 Bardeen J.M., Bond J.R., Kaiser N., Szalay A.S., 1986, *ApJ*, 304, 15
 Binney J., Tremaine S., 1987, *Galactic Dynamics*, Princeton
 Chandrasekhar S., 1943, *ApJ*, 97, 255
 Colpi M., Mayer L., Governato F., 1999, *ApJ*, 525, 720
 Cora S.A., Muzzio J.C., Vergne M.M., 1997, *MNRAS*, 289, 253
 Danby J.M.A., Bray T.A., 1967, *AJ*, 72, 219
 Efstathiou G., 2000a, *astro-ph/0002245*
 Efstathiou G., 2000b, *astro-ph/0002249*
 Ghigna S., Moore B., Governato F., Lake G., Quinn T., Stadel J., 1998, *MNRAS*, 300, 146
 Ghigna S., Moore B., Governato F., Lake G., Quinn T., Stadel J., 1999, *astro-ph/9910166*
 Hannestad S., Scherrer R.J., 2000, *astro-ph/0003046*
 Heisler J., White S.D.M., 1990, *MNRAS*, 243, 1998
 Klypin A.A., Gottlöber S., Kravtsov A.V., Khokhlov A.M., 1999a, *ApJ*, 516, 530
 Klypin A.A., Kravtsov A.V., Valenzuela O., Prada F., 1999b, *astro-ph/9901240*
 Mateo M., 1998, *ARA&A*, 36, 435
 Moore B., Katz N., Lake G., 1996, *ApJ*, 457, 455
 Moore B., Ghigna S., Governato F., Lake G., Quinn T., Stadel J., Tozzi P., 1999, *ApJ*, 524, L19
 Moore B., Gelato S., Jenkins A., Pearce F.R., Quilis V., 2000, *astro-ph/0002308*
 Mulder W.A., 1983, *A&A*, 117, 9
 Okamoto T., Habe A., 1999, *ApJ*, 516, 591
 Percival W., Miller L., 1999, *MNRAS*, 309, 823
 Saslaw W.C., 1985, *Gravitational physics of stellar and galactic systems*, Cambridge
 Sommer-Larsen J., Dolgov A., 1999, *astro-ph/9912166*
 Spergel D., Steinhardt P., 1999, *astro-ph/9909386*
 Tormen G., Diaferio A., Syer D., 1998, 299, 728
 Tóth G., Ostriker J.P., 1992, *ApJ*, 389, 5
 Tremaine S., 1976, *ApJ*, 203, 72
 Yoshida N., Springel V., White S.D.M., Tormen G., 2000, *astro-ph/0002362*
 van den Bosch F.C., Lewis G.F., Lake G., Stadel J., 1999, *ApJ*, 515, 50
 van Kampen E., 1995, *MNRAS*, 273, 295
 van Kampen E., 2000, submitted to *MNRAS*, *astro-ph/0002027*
 Weinberg M.D., 1989, *MNRAS*, 239, 549
 White S.D.M., 1976, *MNRAS*, 174, 467
 White S.D.M., 1996, in Schaeffer et al., eds., *Cosmology and Large-scale structure*, Proc. 60th Les Houches School, Elsevier, p.349
 Zaritsky D., White S.D.M., 1988, *MNRAS*, 235, 289